Electrical Power and Energy Systems 161 (2024) 110209

Contents lists available at ScienceDirect

International Journal of Electrical Power and Energy Systems

journal homepage: www.elsevier.com/locate/ijepes

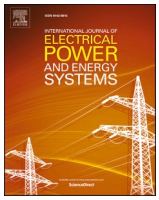

Time-of-use (TOU) electricity rate for vehicle-to-grid (V2G) to minimize a charging station capacity

Jung-Sung Park [a], Shahid Hussain [b], Jin-Oh Lee [c], Balho H. Kim [d], Yun-Su Kim [e,*]

[a] Smart Power Distribution Lab., KEPCO Research Institute, Daejon 34056, South Korea
[b] School of Business, National University of Ireland Maynooth, Ireland
[c] Department of Energy Engineering, Korea Institute of Energy Technology (KENTECH), Naju 58330, South Korea
[d] Department of Electronic and Electrical Engineering, Hongik University, Seoul 04066, South Korea
[e] Graduate School of Energy Convergence, Gwangju Institute of Science and Technology, Gwangju 61005, South Korea

ARTICLE INFO

Keywords:
Electricity rate
Electric vehicle
Installation capacity of a charging station
Modified particle swarm optimization
Vehicle-to-grid

ABSTRACT

This paper introduces a framework to yield an electricity rate for vehicle-to-grid (V2G) charging station (CS) to minimize installation capacity of a charging station considering electric vehicle (EV) arrival/departure time distribution. Two different layers are designed to avoid an obstacle encountered when formulating the problem as a convex optimization and to represent an EV aggregator and an electricity rate decision maker – a regulator. The EV aggregator layer focuses on increasing the profit and the regulator minimizes the peak load of the V2G CS. Linear programming was formulated for the former layer, and a modified particle swarm optimization (PSO) method was developed for the latter. Modification of the PSO approach allowed for easier escape of local minima, resulting in a new electricity rate for the V2G CS based on the EV arrival/departure time distribution data. The algorithm employs new matrices devised in this paper to accommodate EV information in the optimization process. In a simulation study, two distinct CSs with V2G operations were evaluated, each with a different EV arrival/departure time distribution. The simulation revealed that the peak load and the profit of the aggregator vary dramatically depending on the arrival/departure time distributions.

Note that the indices belong to any set are denoted as subscripts, italic, and lowercase letters. Non-italic superscripts describe abbreviations of certain terms – e.g., superscripts ch and di stand for charging and discharging.

1. Introduction

Many countries in Europe and North America have announced plans to phase out the sale and registration of internal combustion engine-powered passenger cars [1]. In 2022, South Korea's president pledged to freeze new registrations of internal combustion engine automobiles beginning in 2035. The rise of electric vehicles (EVs) has created need for more fast-charging stations, given the inconvenience and time costs of long charging queues [2]. The global market for EV fast-charging systems is expected to reach a value of 10.82 billion USD by 2031, increasing at a compound annual growth rate of 16.56 % from 2022 to 2031 [3]. However, plans for new power equipment installations have not been well publicized, such that the proposed timing of implementation is questionable.

In Korea, the maximum capacity of the main feeder is regulated at 10 MVA per circuit by the Korea Electric Power Company (KEPCO) [4]. This value is also applied to the available total capacity of a distributed energy resources (DERs) connection, based on the name plate power rating of the DERs. The maximum number of fast chargers that can be placed on a single main feeder ranges from 50 to 200, with power ratings between 50 and 200 kW [3]. The total capacity of Korean substation transformers is 153,020 MVA [5]; thus, only 765,100–3,060,400 fast chargers may be used simultaneously if no other loads consume electricity. However, the traffic volume per day is about 4,200,000–6,400,000 cars [6], which requires more than the current maximum number of fast chargers that can be installed.

The integration of EVs into the power grid would thus necessitate the installation of new distribution substations and/or substation transformers. However, the cost of establishing a new distribution substation is significant, approaching 1.2 million USD on average [7]. In South Korea, depending on the transformer capacity (30–60 MVA) and distribution line length and type, the total cost ranges from 4,916 million South Korean Won (KRW) to 18,900 million KRW; the total cost

* Corresponding author.
E-mail addresses: jindulfa@kepco.co.kr (J.-S. Park), shahid.hussain@mu.ie (S. Hussain), jolee@kentech.ac.kr (J.-O. Lee), bhkim@hongik.ac.kr (B.H. Kim), yunsukim@gist.ac.kr (Y.-S. Kim).

https://doi.org/10.1016/j.ijepes.2024.110209
Received 26 February 2024; Received in revised form 15 July 2024; Accepted 27 August 2024
Available online 2 September 2024

Nomenclature

Sets and Indices

$\mathscr{I} = \{\forall i \in \mathbb{N}\}$	Set of electric vehicles (EVs)
$\mathscr{J} = \{\forall j \in \mathbb{N}\}$	Set of EV chargers
$\mathscr{T} = \{\forall t \in \mathbb{N}\}$	Set of timeslots
$\mathscr{T}^{\mathrm{a}} = \{\forall t_i^{\mathrm{a}} \in \mathbb{N}\}$	Set of EV arrival timeslots
$\mathscr{T}^{\mathrm{d}} = \{\forall t_i^{\mathrm{d}} \in \mathbb{N}\}$	Set of EV departure timeslots
$\mathscr{S} = \{\forall s_i \in \mathbb{R}\}$	Set of initial state-of-charges (SOCs) of EVs
$\mathscr{R} = \{\forall r \in \mathbb{Z}\}$	Set of time-of-use (TOU) electricity rate indices: $r = 0/1/2$ for off-peak/mid-peak/peak time
$\mathscr{I}_t^{\mathrm{o}}$	Set of online EVs time t
$\mathscr{I}_t^{\mathrm{a/d}}$	Set of arrival/departure EVs at time t
$\mathscr{T}^{\mathrm{o/m/p}}$	Set of off-peak/mid-peak/peak timeslots

Parameters

Δt	Unit time interval [hour]
$\eta^{\mathrm{ch/di}}$	Charging/discharging efficiency [%]
κ^{dcom}	Discomfort rate of EV owner [KRW]
$\gamma_{1/2}$	Acceleration constants for PSO algorithm
$\rho_{1/2}$	Random numbers in range [0, 1] for PSO algorithm
$\overline{E}_i$	Energy rating of EV i [kWh]
$\overline{P}_i$	Power rating of EV i [kW]
$\underline{SOC}$	Minimum SOC of EV [%]
$\overline{SOC}$	Maximum SOC of EV [%]
N^{iter}	Number of iterations for PSO algorithm
N^{pop}	Number of populations for PSO algorithm
N^{var}	Number of variables for PSO algorithm
$\overline{N^{\mathrm{cnt}}}$	Maximum number of counts of consecutive iterations with the same $\boldsymbol{X}^{\mathrm{gbest}}$ in the PSO algorithm
$\mathbf{C}$	EV connection matrix
$c_{i,t}$	ith row, tth column element of $\mathbf{C}$: 1 if EV i is connected to a charger at time t, 0 otherwise
$\mathbf{O}$	Charger occupation matrix
$o_{j,t}$	jth row, tth column element of $\mathbf{O}$: i if EV i is connected to charger j at time t, 0 otherwise

Variables

s_i	Initial SOC of EV i, random variable
$t_i^{\mathrm{a/d}}$	Arrival/departure time of EV i, random variables
$n^{\mathrm{o/m/p}}$	Number of off-peak/mid-peak/peak time indices in $\mathscr{R}$
$u_{i,t}^{\mathrm{ch/di}}$	Charging/discharging status of EV i: 1 if EV i is charging/discharging, 0 otherwise
$p_{i,t}^{\mathrm{ch/di}}$	Charging/discharging power of EV i at time t [kW]
$e_{r,t}^{\mathrm{ch/di}}$	Charging/discharging electricity rate with rate index r at time t [KRW]
$soc_{i,t}$	SOC of EV i at time t [%]

comprises transformer and distribution line construction costs, as well as social, maintenance, and environmental costs [8]. According to a simulation study [9], even substituting 10 % of conventional vehicles with EVs might produce unacceptable voltage fluctuations in a distribution network.

Given the 25,350,000 cars, including 300,000 EVs, registered in Korea at the end of the third quarter of 2022 [10], one of the most important issues for EV adoption is decreasing the power rating of EV charging stations (CSs), as evidenced by the numerous solutions for EV grid integration problems proposed in the literature.

A methodological framework for plug-in EVs scheduling considering uncertainties was introduced in [11]. In addition to uncertain departure time and time-of-use (TOU) price rates, optimal charging timing for EVs was considered in [12]. In [13], an optimum EV charging scheduling problem for co-CSs is defined to reduce overall charging costs. In [14], a conic optimization strategy for EV charging scheduling is proposed with consideration of battery voltage constraints. Many different approaches for reducing the peak load have also been proposed [15–21]. However, all of the solutions are centered on EV charging schedules, which typically have specific objectives such as profit maximization or peak load reduction throughout the whole power grid. These objectives prevent minimization of the power rating of each CS. Given that EV owners and CS operators are interested only in maximizing profits, price tariffs should be modified to encourage a reduction in CS capacity.

Few studies have been conducted on the pricing tariffs for EV charging. The overall costs of fueling plug-in hybrid EVs are compared in [22] using predicted and real-world TOU rates, with the goal of maximizing each consumer's profit. However, when EVs are managed by an aggregator, the overall profit might be enhanced. It has been demonstrated that aggregating EVs through an aggregator and participating in market services may increase the overall benefit for EV owners [23,24]. To lessen the daily load pattern's peak-valley disparity, a novel time series of the TOU technique is suggested in [25]; however, the study focused on the entire power system rather than the peak of a single CS. Furthermore, it did not take into account the optimal charging schedule for EVs.

Many more studies have been conducted on EVs for different reasons, including approaches for optimizing the location and size of EV CSs [26–29]. The research in [30–32] concentrated on reducing grid effects, whereas in [15,33,34] the authors evaluated reducing billing costs for all stakeholders. However, no study has examined optimal EV charging price tariffs to reduce each CS's power rating.

In this paper, a framework for acquiring optimal vehicle-to-grid (V2G) CS electricity rate is introduced to minimize the installation capacity of a V2G CS for the regulator. We considered the regulator since the regulator 1) designs ((or at least approves) a new electricity tariff, and 2) endeavours to maximize social welfare, a goal impacted by network expansion investments [35] – minimizing the installation capacity of each CS helps deferring the network expansion. Two different layers are introduced to acquire a new electricity rate. The first layer depicts the optimization for an EV aggregator and defines the objective to maximize the aggregator's profit under current TOU rate conditions. The second layer reduces the peak load of a CS by adjusting the TOU rates. The peak load is chosen as the objective function for this layer since it is the most relevant factor to the installation capacity of a CS. Several probability distribution functions for EV departure and arrival times were applied; their parameters changed depending on the location of the CS (e.g., residential area, workplace, etc.). The simulation results showed that the TOU rate should be calculated based on the arrival and departure times of EVs at a CS, rather than the entire power system load profile, which is typically used to estimate the TOU rate. In the perspective of the regulators, they don't have to ask or get any kind of information or data from the aggregator. They only need a representative EV arrival/departure time distribution for a certain type of CS, e.g., workplace and residential area, which can be acquired from open data platform. The contributions of this paper are summarized in the following:

- An optimization framework is introduced to determine the new electricity rate, considering demand-side power capacity limitations. The proposed framework can solve the problem which cannot be formulated as a standard bi-level convex optimization.
- Algorithms to determine optimal TOU price for each time slot considering the arrival/departure time distribution of EVs are developed, which has been barely studied previously.

- An EV connection matrix was developed to make charging/discharging scheduling algorithm implementation much easier.
- The modified particle swarm optimization (PSO) algorithm increases the convergence rate of the algorithm.
- Simulation results revealed that the TOU rates for EV CSs should be adjusted according to EV arrival/departure time distribution.

We used known optimization and simple uncertainty models in this paper since we focus on regulators to easily adopt mathematically comprehensible method and hence to deploy a new electricity tariff for EV CSs in the real-world. Deployment of a new electricity tariff is especially urgent in South Korea, which has 1) no grid interconnection with surrounded countries to support the grid, 2) no surplus area to expand the grid, and 3) aggressive EV penetration plans as mentioned at the beginning of this section.

The remainder of this paper is organized as follows. Section 2 depicts the overall framework of the optimization technique. Section 3 provides algorithms for each layer. The simulation environment and results are described in Section 4. Section 5 summarizes the findings of this paper.

2. Optimization problem formulation

2.1. Problem statement

The objective of the regulator is to solve the problem of the minimization of a daily peak load as follow:

$$\min_{r\in\mathscr{R}}\max\left\{\begin{array}{c}\left|\sum_{i\in\mathscr{I}}p_{i,1}^{\mathrm{ch}}-p_{i,1}^{\mathrm{di}}\right|,\left|\sum_{i\in\mathscr{I}}p_{i,2}^{\mathrm{ch}}-p_{i,2}^{\mathrm{di}}\right|,\\ \ldots,\left|\sum_{i\in\mathscr{I}}p_{i,T}^{\mathrm{ch}}-p_{i,T}^{\mathrm{di}}\right|\end{array}\right\} \tag{1}$$

where T is the terminal timeslot index and is also equivalent to the cardinality of $\mathscr{T}$, $|\mathscr{T}|$. Note that 'min.' stands for 'minimize' and 'max' denotes the max function, which selects the maximum value among a list and is a convex function [36]. However, the values in the max function cannot be explicitly expressed by using r, which is the TOU rate index (decision variable) for the regulator's problem (minimization problem) and has discrete values. Even if the price itself is set as the decision variable instead of the index, the problem remains the same since the prices are discrete values which are not integers nor real numbers as shown in Table 1. Hence, (1) cannot be formulated as a convex function. In order to relate r and $p_{i,t}^{\mathrm{ch/di}}$, the EV aggregator is introduced and its objective is to minimize the operation cost (or maximization of the profit) of the CS as follow (the details are discussed in Section 2.3):

$$\min_{p_{i,t}^{\mathrm{ch}},p_{i,t}^{\mathrm{di}}} OC \tag{2}$$

$$OC=\sum_{i\in\mathscr{I}}\left\{\begin{array}{c}\sum_{t\in\mathscr{T}}c_{i,t}\Delta t\left(p_{i,t}^{\mathrm{ch}}e_{r,t}^{\mathrm{ch}}-p_{i,t}^{\mathrm{di}}e_{r,t}^{\mathrm{di}}\right)\\ +\kappa^{\mathrm{dcom}}\left(\overline{SOC}-soc_{i,t_i^{\mathrm{d}}}\right)\end{array}\right\} \tag{3}$$

In order to formulate a complete bi-level (the regulator level and the EV aggregator level) convex optimization problem, (2) and (3) should be incorporated into (1). However, it is unable to merge them without losing convexity. Hence, an optimization framework to solve this problem is proposed.

Table 1
KEPCO TOU rate for EV charging in summer.

Voltage level	Option[a]	Demand charge (KRW/kW)	Time regarding load level[b]	Energy charge (KRW/kWh)
Medium voltage	II	2,580	Off-peak	51.4
			Mid-peak	86.2
			Peak	171.8

[a] There are several more options with different demand and energy charges.
[b] In summer, off-peak time is 23:00–09:00, mid-peak time is 09:00–10:00, 12:00–13:00, and 17:00–23:00, and peak time is 10:00–12:00, and 13:00–17:00.

2.2. Optimization framework

The electricity rate for the V2G CS is acquired by employing the optimization framework depicted in Fig. 1. One layer is an EV aggregator optimization (EAO) layer, which yields the optimal charging/discharging schedule for each EV to maximize EV aggregator profit while minimizing EV owner discomfort by fully charging the battery before departure. The EAO layer is responsible for determining the optimal charge/discharge schedule, which results in a convex optimization problem that can be solved using linear programming (LP) [32].

The other layer is an electricity rate optimization (ERO) layer, which establishes a new electricity rate by implementing the PSO algorithm to minimize the peak load demand of the V2G CS. Moreover, the EAO acts as a fitness function that outputs the peak load demand to the PSO algorithm at a given electricity rate. The PSO algorithm is applied because the relationship between the electricity rate and peak load demand cannot be modeled as a convex function. Hence, both layers cannot be combined into a single minimax problem. One downside of the PSO algorithm is that it cannot mathematically guarantee a global optimum; consequently, in Section 3, we suggest a modified PSO algorithm to address this issue.

The modified PSO algorithm attempts to reduce peak load demand by allocating one of three rates to each timeslot: off-peak, mid-peak, or on-peak. The EV charging TOU rate is based on the KEPCO EV charging rate in summer [37]; the details are presented in Table 1. Given the daily load activities, the temporal horizon is discretized into 24 h with 1-h timeslots. Following the data in Table 1, 10 timeslots are designated as off-peak times, 8 as mid-peak times, and 6 as on-peak times for each day.

Adopting the electricity rate as a decision variable may enhance the flexibility of the problem, thereby allowing the electricity rate to be divided into more than three levels and/or to be increased to excessively expensive price. To limit the degree of freedom of the electricity rate as the decision variable, the following assumptions were applied:

- There are only three types of times – off-peak, mid-peak, and peak times.
- Each time slot has a constant energy charge.
- The numbers of off-peak, mid-peak, and peak timeslots (10, 8, and 6, respectively) stay the same.

According to these assumptions, only the time intervals between each load level can be exchanged. For instance, if the time interval 23:00–24:00 is changed from off-peak to on-peak, only one of the on-peak time intervals must be changed to the off-peak time. Changing the time of the load level is reasonable because the current TOU rate is based on the national load pattern of South Korea, whereas the load of the EV station may differ.

For the V2G system, the price rates for selling electricity from EVs are also required. However, the current electricity rate does not provide the price rates for selling. Thus, we assumed that the electricity price for selling is 130 % of the TOU rates in Table 1, given that approximately 124 % ($1.24 \approx 1/0.9/0.9$, where 90 % is the charging/discharging efficiency) is the minimum rate that enables the EV aggregator to make a profit considering the charging/discharging efficiency. If the selling price is less than 124 % of the buying price, the EVs will never be discharged since they cannot recover the power losses in converters and batteries. On the other hand, higher selling price would result economic inefficiency for the utility. Investigation of a proper upper level of the electricity selling price for the V2G is worthwhile to be discussed as a new research topic. It is out of scope of this paper since higher electricity

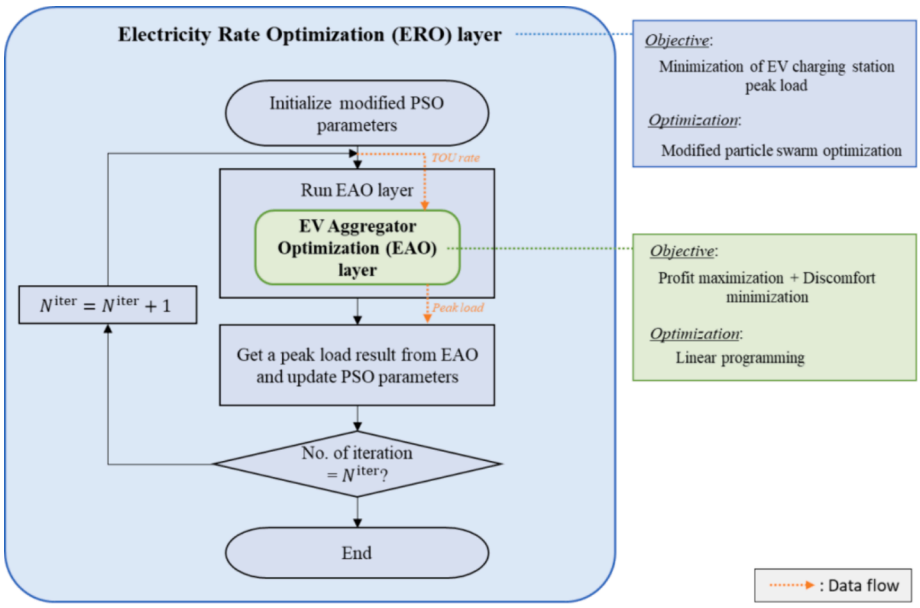

Fig. 1. A proposed framework to yield a new electricity rate for V2G CS peak load minimization.

selling price would not yield a different result if EVs are subjected to be fully charged before they leave, which can be implemented by considering the discomfort rate of EV owners.

2.3. Objective functions and constraints

The EAO problem is formulated as an LP problem with the objective function as (2) and (3), where $r \in \mathscr{R}$ is the TOU rate calculated from the ERO layer. The V2G CS operating cost minimization is defined in (2) and further detailed in (3). It includes the total cost of purchasing electricity (first term), total cost of selling electricity (second term), and total discomfort cost for EV owners (last term). The EV connection indicator $c_{i,t}$ is a predefined (i.e., non-variable) parameter calculated by the EV arrival/departure time distribution generator, as detailed in Section 3. The discomfort cost is the aggregate of all EV owners' discomfort levels, and it is represented by the greatest discomfort level of an ith EV owner if the SOC at departure time t_i^{d} deviates significantly from the $\overline{SOC}$ level. The discomfort rate κ^{dcom} is set at 200 KRW, which means that for every 1 % SOC deviation from the maximum value, it costs 200 KRW. However, due to its temporal-spatial variability, accurately estimating the cost for EV owners' discomfort is extremely difficult. For instance, a AAA battery costs 10,000 times more than the same amount of energy from the power grid [38]. However, the discomfort rate is intended to be higher than the average electricity rate in South Korea, which is around 100 KRW/kWh.

The charging/discharging of EVs is constrained as ($\forall t \in \mathscr{T}$, $\forall i \in \mathscr{I}$):

$$0 \le p_{i,t}^{\mathrm{ch}} \le c_{i,t} u_{i,t}^{\mathrm{ch}} \overline{P}_i \tag{4a}$$

$$0 \le p_{i,t}^{\mathrm{di}} \le c_{i,t} u_{i,t}^{\mathrm{di}} \overline{P}_i \tag{4b}$$

$$0 \le u_{i,t}^{\mathrm{ch}} + u_{i,t}^{\mathrm{di}} \le 1 \tag{4c}$$

$$\underline{SOC} \le soc_{i,t} \le \overline{SOC} \tag{4d}$$

$$soc_{i,t} = soc_{i,t-1} + \frac{c_{i,t}\Delta t}{\overline{E}_i}\left(\eta^{\mathrm{ch}} p_{i,t}^{\mathrm{ch}} - p_{i,t}^{\mathrm{di}}/\eta^{\mathrm{di}}\right) \tag{4e}$$

where $soc_{i,t} = 0$ for $t < t_i^a$ and $soc_{i,t_i^a} = s_i \in \mathscr{S}$. Since t_i^{d}differs between each EV, acquiring $soc_{i,t_i^{\mathrm{d}}}$ in (3) for each EV is quite laborious in terms of algorithm implementation; however, incorporating $c_{i,t}$, greatly simplifies the process, as $t > t_i^{\mathrm{d}}$ and $\forall i \in \mathscr{I}$, $c_{i,t} = 0$. Hence, from (4e), $soc_{i,t_i^{\mathrm{d}}} = soc_{i,T}$. Therefore, instead of obtaining every t_i^{d} to calculate $soc_{i,t_i^{\mathrm{d}}}$ in (3), we can use $soc_{i,T}$, $\forall i \in \mathscr{I}$.

The ERO problem is reformulated from (1) using the following objective function ($\forall t \in \mathscr{T}$):

$$\min_{r \in \mathscr{R}} \left| PL\left(e_{r,t}^{\mathrm{ch}}, e_{r,t}^{\mathrm{di}}, \mathbf{C}, \mathscr{S}\right) \right| \tag{5}$$

subject to:

$$0 \le r \le 2, \forall r \in \mathbb{Z} \tag{6a}$$

$$n^{\mathrm{o}} = |\mathscr{T}^{\mathrm{o}}|, n^{\mathrm{m}} = |\mathscr{T}^{\mathrm{m}}|, n^{\mathrm{p}} = |\mathscr{T}^{\mathrm{p}}| \tag{6b}$$

Note that (5) is exactly the same problem as (1) but (5) is described as a function of controllable variables and acquirable parameters to the regulator whereas (1) is described as a function of charging/discharging power of EVs at each time interval, which is controlled by the aggregator. So, the peak load of the V2G CS, PL, cannot be described explicitly by using the regulator's decision variable (the electricity rate index). However, the electricity rate directly affects the aggregator's scheduling strategy which yields PL as a result. Consequently, by introducing the EAO (aggregator's) problem, the ERO (regulator's) problem is able to relate the electricity rate and PL. The PSO algorithm is utilized to solve the ERO problem based on the following equations [39]:

$$\boldsymbol{V}_{k+1,l} = \boldsymbol{V}_{k,l} + \gamma_1\rho_1\left(\boldsymbol{X}_{k,l}^{\mathrm{lbest}} - \boldsymbol{X}_{k,l}\right) + \gamma_2\rho_2\left(\boldsymbol{X}^{\mathrm{gbest}} - \boldsymbol{X}_{k,l}\right) \tag{7}$$

$$\boldsymbol{X}_{k+1,l} = \boldsymbol{X}_{k,l} + \boldsymbol{V}_{k+1,l} \tag{8}$$

where $\boldsymbol{V}$ and $\boldsymbol{X}$ are the velocity and the position vectors, respectively, and the superscripts lbest and gbest denote local best and global best, respectively. The element of $\boldsymbol{X}$ consists of r and the size of vectors $\boldsymbol{X}$ and $\boldsymbol{V}$ is $N^{\mathrm{var}} \times 1$. The EAO layer is used to calculate the objective function of the ERO layer as shown in Fig. 1. So, the EAO layer is conducted every iteration of the ERO layer. The iteration of the ERO layer (the modified PSO algorithm) stops when the number of iterations reaches N^{iter}.

The network constraints are not considered in the problem since it is considered by the utility whereas the EAO and the ERO problems represents the aggregator and the regulator, respectively. The utility reviews an available power capacity for the EV CS considering network constraints. Once the available power capacity is determined for the EV

CS, the aggregator must not exceed the capacity while they manage the EV CS. Hence, in this paper, we did not incorporate the network constraints, which is the utility's concern, into the electricity tariff decision problem, which is the regulator's concern or into the EV charging/discharging scheduling problem, which is the aggregator's concern.

3. Algorithms

3.1. EAO layer

Algorithm 1 Generation of charger occupation matrix **O**

Input: $\mathscr{T}^{a/d}$, $|\mathscr{J}|$, $|\mathscr{T}|$
Output: Charger occupation matrix **O**

01:Initialize **O** as $|\mathscr{J}|$ by $|\mathscr{T}|$ zero matrix
02:**for** $t \leftarrow 1$ to $|\mathscr{T}|$ **do**
03:Compute $\left|\mathscr{J}_t^{a/d}\right|$ // number of EV arr./dep. at t
04:**if** $(\left|\mathscr{J}_t^{d}\right| > 0)$ **then**
05:Extract $\mathscr{J}_t^{d}$ randomly among $\mathscr{J}_{t-1}^{o}$
06:**for** $j \leftarrow 1$ to $|\mathscr{J}|$ **do**
05:Choose i randomly from $\mathscr{J}_t^{d}$
07:**if** $(\mathbf{O}[j,t] == i \in \mathscr{J}_t^{d})$ **then** ▶ *If j is occupied*
08: $\mathbf{O}[j,t] \leftarrow 0$ ▶ *Mark j as empty*
09:Remove i from $\mathscr{J}_t^{d}$
10: **end if**
11: **end for**
12:**else if** $(\left|\mathscr{J}_t^{a}\right| > 0)$ **then**
13Get $\mathscr{J}_t^{a}$ from $\left(\bigcup_{x=1}^{t-1}\mathscr{J}_x^{a}\right)^{C}$
14:**for** $j \leftarrow 1$ to $|\mathscr{J}|$ **do**
15:**if** $(\mathbf{O}[j,t] == 0)$ **then**▶ *If j is empty*
16:$\mathbf{O}[j,t] \leftarrow i \in \mathscr{J}_t^{a}$▶ *Assign EV i to charger j*
17:Remove i from $\mathscr{J}_t^{a}$
18:**end if**
19: **end for**
20:**end if**
21:**end for**

To solve the EAO problem deterministically, probability density functions (PDFs) are employed to generate the EV arrival/departure timeslots and EV SOCs at the arrival time before running the EAO problem. Since we focus on the types (e.g., workplace, residential area, and so on) of V2G TOU price, the PDF can be used to represent the pattern of many, but same types of loads instead of a specific pattern of a single load. The PDFs of the EV arrival and departure times are referred to in [11] and [40] with slight modification, which gives the Weibull distribution $\mathscr{T}^{d} \sim \mathrm{W}(k,\lambda)$ and generalized extreme value (GEV) distribution $\mathscr{T}^{a} \sim \mathrm{G}(\mu,\sigma,\xi)$, where μ is the location parameter, σ and k are shape parameters, and ξ and λ are scale parameters. The PDF of EV SOCs at the arrival time is modeled as a normal distribution function $\mathscr{S} \sim \mathrm{N}(\mu_N, \sigma_N)$, where μ_N and σ_N are the mean and standard deviation of the normal distribution, respectively. However, depending on the on-site statistics, any alternative distribution function can replace these distribution functions. The details of the PDFs are discussed in Section 4.

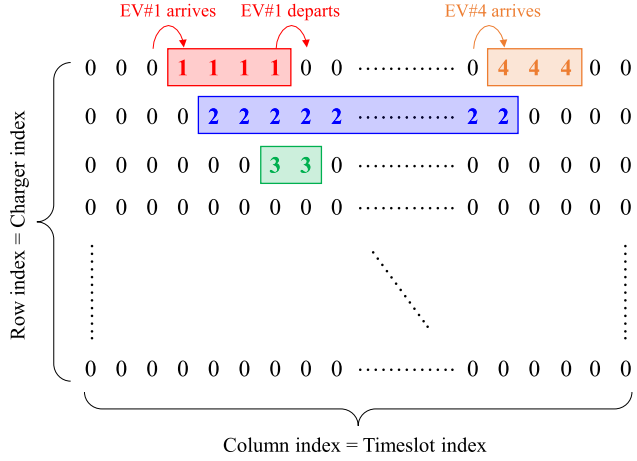

Fig. 2. Illustration of the charger occupation matrix **O**.

The data extracted from the PDFs are input into the algorithm that generates charger occupation matrix **O**; the algorithm's pseudocode is shown in Algorithm 1. In Algorithm 1, one of the input $\mathscr{T}^{a/d}$ is extracted from PDFs of EV arrival/departure times under the assumption that $|\mathscr{T}^{a}| = |\mathscr{T}^{d}| = |\mathscr{J}|$. Note that $\bigcup_{\forall t\in\mathscr{T}}\mathscr{J}_t^{a} = \bigcup_{\forall t\in\mathscr{T}}\mathscr{J}_t^{d} = \mathscr{J}$, and $\mathscr{J}_t^{a} \subseteq \left(\bigcup_{x=1}^{t-1}\mathscr{J}_x^{a}\right)^{C}$. In Line 03, the algorithm computes $\left|\mathscr{J}_t^{a/d}\right|$ by counting the number of identical values in $\mathscr{T}^{a/d}$, such that $\mathscr{T}^{a} = \{1,1,2,2,2\}$ means that $\left|\mathscr{J}_{t=1}^{a}\right| = 2$ and $\left|\mathscr{J}_{t=2}^{a}\right| = 3$. In Line 05, $\mathscr{J}_t^{d}$ is extracted randomly from $\mathscr{J}_{t-1}^{o}$, where $\mathscr{J}_t^{d} \subseteq \mathscr{J}_{t-1}^{o}$ and $\mathscr{J}_{t-1}^{o} = \left(\bigcup_{x=1}^{t-1}\mathscr{J}_x^{a} - \bigcup_{x=1}^{t-1}\mathscr{J}_x^{d}\right)$. The row and column indices of **O** represent the EV charger and timeslot, respectively. The value of an element of **O** is i if the charger j (=row index) is occupied by the ith EV at time t (=column index), and 0 if the charger is empty.

Algorithm 2 Generation of EV connection matrix **C**

Input: **O**, $|\mathscr{J}|$, $|\mathscr{J}|$, $|\mathscr{T}|$
Output: EV connection matrix **C**

01:Initialize **C** as $|\mathscr{J}|$ by $|\mathscr{T}|$ zero matrix
02:**for** $i \leftarrow 1$ to $|\mathscr{J}|$ **do**
03:**for** $j \leftarrow 1$ to $|\mathscr{J}|$ **do**
04:**for** $t \leftarrow 1$ to $|\mathscr{T}|$ **do**
05:**if** $(\mathbf{O}[j,t] == i)$ **then**
06:$\mathbf{C}[i,t] \leftarrow 1$▶ *EV plugged in*
07: **else**
08$\mathbf{C}[i,t] \leftarrow 0$▶ *EV plugged off*
07:**end if**
08:**end for**
09:**end for**
10:**end for**

Algorithm 2 provides the pseudocode for generating the EV connection matrix **C**, which takes as input matrix **O** and the terminal values $|\mathscr{J}|$, $|\mathscr{J}|$, and $|\mathscr{T}|$. The row and column indices of **C** denote the EV and timeslot, respectively. The value of an element of **C** is 1 if the EV i (=row index) is occupying the charger at time t (=column index), and 0 if the EV i is not occupying the charger (i.e., the EV i has not arrived yet or has already left the charger). Illustrations of matrices **O** and **C** are shown in Figs. 2 and 3, respectively.

3.2. ERO layer

The objective of the ERO layer is to minimize the peak load PL of the V2G CS, which is acquired from the E-AO result. The PSO algorithm is utilized because the connection between the control variable r and objective function (5) cannot be expressed explicitly. However, the applied heuristic optimization algorithm, i.e., the PSO, has the problem of being stuck in a local minimum; hence, a modified PSO algorithm is presented. The modified PSO algorithm's pseudocode is illustrated in Algorithm 3, where the bold line numbers (05–13, 15, 18–21, and 23–31) emphasize the modified parts of the original algorithm.

Algorithm 3 Modified PSO algorithm

Input: PL, N^{iter}, N^{pop}, N^{var}
Output: $\boldsymbol{X}$ $(=\mathscr{R})$

01:Initialize PSO parameters
02:$count \leftarrow 0$
03:**for** $k \leftarrow 1$ to N^{iter} **do**
04:Update $\boldsymbol{V}_k$, $\boldsymbol{X}_k$▶ *According to (5) and (6)*

(*continued on next page*)

(*continued*)

Algorithm 3 Modified PSO algorithm

05:for $m \leftarrow 1$ to N^{var} **do**
06:for $l \leftarrow 1$ to N^{pop} **do**
07:if ($X_{k,l,m} > \overline{X_m}$) **then**
08:$X_{k,l,m} \leftarrow \overline{X_m}$
09:else if ($X_{k,l,m} < \underline{X_m}$) **then**
10:$X_{k,l,m} \leftarrow \underline{X_m}$
11:end if
12:end for
13:end for
14:**for** $l \leftarrow 1$ to N^{pop} **do**
15:$\boldsymbol{X}_{k,l} \leftarrow$ **Recount_TOU_Rate**(*arguments*)
16:Compute *PL* by running the EAO layer
17:Update $\boldsymbol{X}_{k,l}^{\text{lbest}}$, $\boldsymbol{X}^{\text{gbest}}$
18:if ($\boldsymbol{X}^{\text{gbest}} == \boldsymbol{X}_{k,l}^{\text{lbest}}$) **then**
19: Initialize $\boldsymbol{X}_{k,l}$
20:$\boldsymbol{X}_{k,l} \leftarrow$ **Recount_TOU_Rate**(*arguments*)
21:end if
22:**end for**
23:if ($\boldsymbol{X}^{\text{gbest}} == \boldsymbol{X}_k^{\text{gbest}}$) **then**
24:*count* ← *count* + 1
25:if (*count* == $\overline{N^{\text{cnt}}}$) **then**
26:*count* ← 0
27: Initialize randomly chosen half particles in $\boldsymbol{X}_k$
28:end if
29:else if ($\boldsymbol{X}^{\text{gbest}}! = \boldsymbol{X}_k^{\text{gbest}}$) **then**
30:*count* ← 0
31:end if
32:**end for**

The first modified part (Lines 05–13) implements the constraint condition (6a) by constraining the element X of position vector $\boldsymbol{X}$ within lower and higher limits, $\underline{X}$ and $\overline{X}$, respectively. Since $X = r \in \{0, 1, 2\}$, $\underline{X}$ and $\overline{X}$ are 0 and 2, respectively. It is worth noting that X s are integers, but the updates of $\boldsymbol{V}$ and $\boldsymbol{X}$ provide real numbers for X s. To make X s integers and hence implement integer PSO, they are rounded down to the nearest integer in every update and initialization. Likewise, the second amended component (Line 15) is intended to confine $n^{\text{o/m/p}}$ so that it is comparable to $|\mathscr{T}^{\text{o/m/p}}|$, to execute the constraint condition (6b). According to Table 1, $|\mathscr{T}^{\text{o}}|$, $|\mathscr{T}^{\text{m}}|$, and $|\mathscr{T}^{\text{p}}|$ are 10, 8, and 6, respectively, whereas n^{o}, n^{m}, and n^{p} can be adjusted during the PSO algorithm's solution searching process. To reset $n^{\text{o/m/p}}$ to $|\mathscr{T}^{\text{o/m/p}}|$, the **Recount_TOU_rate** algorithm is created and used at Lines 15 and 20, where the pseudocode of the **Recount_TOU_rate** algorithm is presented in Algorithm 4. The algorithm takes inputs $|\mathscr{T}^{\text{o}}|$, $|\mathscr{T}^{\text{m}}|$, $|\mathscr{T}^{\text{p}}|$, and $\boldsymbol{X}$ ($=\mathscr{R}$) and counts n^{p} whichcould be different from $|\mathscr{T}^{\text{p}}|$. If $n^{\text{p}} > |\mathscr{T}^{\text{p}}|$, the algorithm changes $n^{\Delta\text{p}}$ ($= |n^{\text{p}} - |\mathscr{T}^{\text{p}}||$) '2's (peak-time indices) in $\mathscr{R}$ into '0's (off-peak time indices), whereas if $n^{\text{p}} < |\mathscr{T}^{\text{p}}|$, the algorithm changes $n^{\Delta\text{p}}$ '0's and '1's (mid-time indices) in $\mathscr{R}$ into '2's. Then, the algorithm counts n^{m}, which could be different from $|\mathscr{T}^{\text{m}}|$. If $n^{\text{m}} > |\mathscr{T}^{\text{m}}|$, the algorithm changes $n^{\Delta\text{m}}$ ($= |n^{\text{m}} - |\mathscr{T}^{\text{m}}||$) '1's in $\mathscr{R}$ into '0's. If $n^{\text{m}} < |\mathscr{T}^{\text{m}}|$, the algorithm changes $n^{\Delta\text{m}}$ '0's and '2's in $\mathscr{R}$ into '1's. Eventually, $n^{\text{o/m/p}}$ become equivalent to $|\mathscr{T}^{\text{o/m/p}}|$.

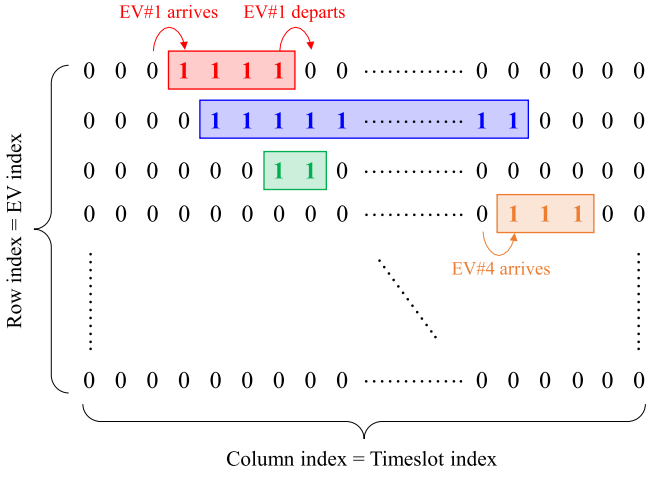

Fig. 3. Illustration of the EV connection matrix **C**.

Algorithm 4 Recount_TOU_Rate(*arguments*)

Input: $|\mathscr{T}^{\text{o}}|$, $|\mathscr{T}^{\text{m}}|$, $|\mathscr{T}^{\text{p}}|$, $\boldsymbol{X}$ ($=\mathscr{R}$)
Output: $\boldsymbol{X}$ ($=\mathscr{R}$with n^{o}, n^{m}, and n^{p} recounted)

01:$n^{\text{p}} \leftarrow$ Number of peak time indices in $\mathscr{R}$
02:$n^{\Delta\text{p}} \leftarrow |n^{\text{p}} - |\mathscr{T}^{\text{p}}||$
03: **if** ($n^{\text{p}} > |\mathscr{T}^{\text{p}}|$) **then**
04:Randomly choose $n^{\Delta\text{p}}$ '2's in $\mathscr{R}$
05:Change chosen '2's into '0's in $\mathscr{R}$
06:**else if** ($n^{\text{p}} < |\mathscr{T}^{\text{p}}|$) **then**
07:Randomly choose $n^{\Delta\text{p}}$ '0's and '1's in $\mathscr{R}$
08:Change chosen '0's and '1's into '2's in $\mathscr{R}$
09:**end if**
10:$n^{\text{m}} \leftarrow$ Number of mid-peak time indices in $\mathscr{R}$
11: $n^{\Delta\text{m}} \leftarrow |n^{\text{m}} - |\mathscr{T}^{\text{m}}||$
12:**if** ($n^{\text{m}} > |\mathscr{T}^{\text{m}}|$) **then**
13:Randomly choose $n^{\Delta\text{m}}$ '1's in $\mathscr{R}$
14:Change chosen '1's into '0's in $\mathscr{R}$
15:**else if** ($n^{\text{m}} < |\mathscr{T}^{\text{m}}|$) **then**
16:Randomly choose $n^{\Delta\text{m}}$ '0's and '2's in $\mathscr{R}$
17:Change chosen '0's and '2's into '1's in $\mathscr{R}$
18:**end if**
19:Return updated $\mathscr{R}$

The third modified part of the PSO algorithm (Lines 18–21) aims to maximize particle resource utilization. This section initializes the lth particle $\boldsymbol{X}_l$, which reaches $\boldsymbol{X}^{\text{gbest}}$ since leaving $\boldsymbol{X}_l$ near $\boldsymbol{X}^{\text{gbest}}$ is ineffective. Since every particle is heading toward $\boldsymbol{X}^{\text{gbest}}$, $\boldsymbol{X}_l$ can seek an entirely new region, thereby enhancing the particle's utilization and assisting other particles to escape from local minima.

The fourth updated section (Lines 23–31) is also intended to allow particles to avoid local minima, and it counts the number of successive iterations with the same $\boldsymbol{X}^{\text{gbest}}$. If the number of counts reaches $\overline{N^{\text{cnt}}}$, which is set by the user, half of the particles in $\boldsymbol{X}$ are picked at random and initialized to seek a new region.

The convergence rate to the global optimum is boosted by developing and employing the third and fourth modified parts of the PSO algorithm. To demonstrate the efficiency of the modified PSO algorithm, the original PSO algorithm and genetic algorithm (GA) are developed and applied to an example problem with the same constraints as the ERO problems (6a) and (6b). The Appendix provides the details of the example problem. Three algorithms are used in the example problem, where $N^{\text{iter}} = 2{,}000$, and they stop iterating once they hit the global optimum. The global optimum value is 106, as illustrated in the Appendix. The performance of the three algorithms is compared in Fig. 4 and Table 2. The simulation results are calculated by taking the average, minimum, maximum, and standard deviation of 1,000 distinct algorithm outputs. Only the average value is used for Fig. 4. As shown in Fig. 4(a), the modified PSO outperforms the original one. The GA appears to be quicker than the modified PSO in terms of iteration count. However, as shown in Fig. 4(b), the computational time of the GA is nearly 6.3 times slower than that of the modified PSO and 3.1 times slower than that of the PSO. Furthermore, as shown in Table 2, the GA never approaches the global optimum at iteration number 2,000, whereas the modified PSO reaches the global optimum at iteration number 1,253 at most. In average, by modifying (or by adding the third and fourth modified parts to) the PSO algorithm as proposed, the global optimum value is reduced by 5.4 %. The first and second modified parts cannot be removed because the constraint conditions are violated without them.

Note that the result does not guarantee the effectiveness of the

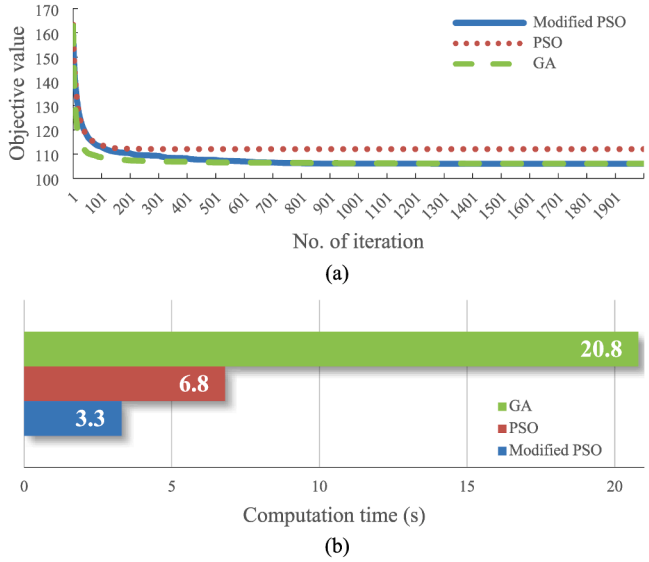

Fig. 4. Performance of the modified PSO, PSO, and GA. (a) Convergence rate. (b) Computation time. (Average values from 1,000 demonstrations).

Table 2
Convergence rate of the modified PSO, PSO, and GA (From 1,000 demonstrations).

	Modified PSO	PSO	GA
Optimum at the terminal iteration: average/min/max/standard deviation	106/106/106/0 (Global optimum)	112.04/107/117/2.13	106.02/106/107/0.14
The largest iteration number that reaches the global optimum	1,253	>2,000	>2,000

modified PSO algorithm for all general optimization problems. The heuristic optimization still cannot be proven for the global optimality mathematically, so the effectiveness check should be done for every problem that could use the modified PSO algorithm. The modified PSO algorithm proposed in this paper is effective for problems with integer variables where the values of variables are under inequality constraint conditions and the number of each integer that should be used are under equality constraint conditions.

The algorithm was evaluated on a computer that has an Intel Core i7 12700 @ 2.1 GHz CPU, 64-bit operating system, and 32 GB of RAM (Intel Corp., Santa Clara, CA, USA).

4. Simulation environment and results

4.1. Simulation environment

The simulation parameters were set to the values shown in Table 3. The V2G CS scheduling algorithm was developed for a 24-h period. $\Delta t = 0.25$ h, so $|\mathscr{T}| = 24/0.25 = 96$ and $\{1, 2, 3, \cdots, 96\} \in \mathscr{T}$. However, $N^{\text{var}} = 24$ since $|\mathscr{T}^{\text{o}}| + |\mathscr{T}^{\text{m}}| + |\mathscr{T}^{\text{p}}| = 24$. As such, the TOU rate indices were imposed on the timeslots on an hourly basis. For instance, timeslots $\{1, 2, 3, 4\}$ have the same TOU rate, as they exist between 0:00 and 1:00. The number of daily EV arrivals was calculated to be 200, which was also deemed equivalent to $|\mathscr{J}|$. Loads other than EV are not considered in order to clearly show how the TOU rate and EV departure/arrival time affect the peak load due to EVs. However, even if the other loads are not considered, it can be inferred that the effect of adding the other load would be the same as changing EV departure/arrival time distribution since both affect a load pattern.

Table 3
Simulation parameters.

Parameters	Values	Units
Δt	0.25	hour
η^{ch}, η^{di}	90, 90	%
κ^{dcom}	200	KRW
$\gamma_{1/2}$	3, 3	–
$\overline{E_i}$	70	kWh
$\overline{P_i}$	50	kW
$\underline{SOC}$, $\overline{SOC}$	0, 100	%
N^{iter}, N^{pop}, N^{var}	2000, 100, 24	–
$\overline{N^{\text{cnt}}}$	100	–

Table 4
PDF parameters.

Random variables	Parameters	Values
$\mathscr{T}^{\text{d}} \sim \text{G}(\mu, \sigma, \xi)$(Residential/Work)	μ	32/72
	σ	–0.05
	ξ	1
$\mathscr{T}^{\text{a}} \sim \text{W}(k, \lambda)$(Residential/Work)	k	7.67
	λ	76/36
$\mathscr{S} \sim \text{N}(\mu_N, \sigma_N)$	μ_N	50
	σ_N	10

The simulation ran two scenarios: one for residential use and the other for the workplace. Each scenario had a completely different distribution of EV arrival and departure times based on the activities taking place there. The random variable sets $\mathscr{T}^{\text{a}}$, $\mathscr{T}^{\text{d}}$, and $\mathscr{S}$ were retrieved from the PDFs with the settings provided in Table 4. The settings were chosen such that $\mathscr{T}^{\text{d}}$ concentrated on the adjacent hours of 8:00 and 18:00 (32 and 72, in terms of timeslots), which correspond to residential area and workplace, respectively. For $\mathscr{T}^{\text{a}}$, they were centered around 19:00 and 9:00 (76 and 36, respectively, in terms of timeslots) for the residential area and workplace, respectively.

The number of EV arrival and departure timeslots at the workplace and residential area are shown in Fig. 5(a) and (b), respectively. We set $|\mathscr{T}^{\text{a}}| = |\mathscr{T}^{\text{d}}| = |\mathscr{J}|, |\mathscr{T}^{\text{a}}| = |\mathscr{T}^{\text{d}}| = 200$. Since the majority of $\mathscr{T}^{\text{d}}$ start before $\mathscr{T}^{\text{a}}$ in the case of the residential area, another 200 EVs were assumed to have been plugged into the chargers since the previous day; hence, they were not created as random variables and are not depicted in Fig. 5(b). These EVs were assumed to be fully charged since $t^{\text{a}} = 1$ and left the residential area at $\mathscr{T}^{\text{d}}$, the distribution of which is shown in Fig. 5(b). The random variable set $\mathscr{T}^{\text{a}}$ is illustrated in Fig. 5(b). The initial SOC random variable set was generated for both the EVs arriving at the residential and workplace locations from the PDF, with the parameters shown in Table 4. The results are shown in Fig. 5(c).

4.2. Simulation results

For both the workplace and residential area, the current TOU electricity rate and rate received from the ERO layer were applied to the EAO layer. It took 51 days and 19 h and 40 min for the workplace case

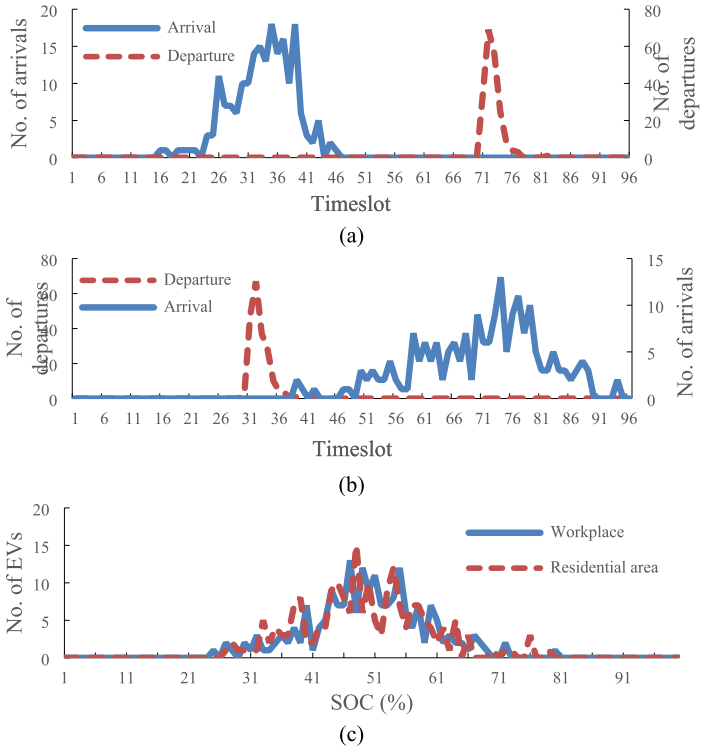

Fig. 5. Number of random variables generated from PDFs. (a) Arrival and departure timeslots for the workplace. (b) Arrival and departure timeslots for residential area. (c) Initial SOCs for EVs.

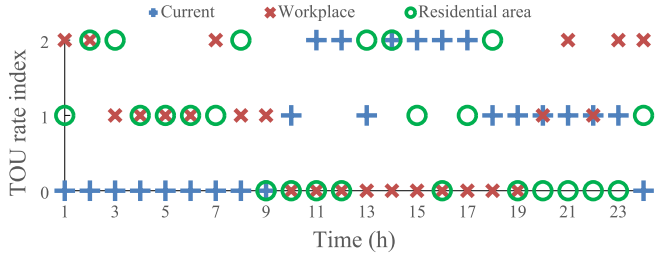

Fig. 6. TOU electricity rate index.

and 74 days and 40 min for the residential area case to get results. Fig. 6 shows the differences in electricity rates and demonstrates that the new electricity rates had completely different patterns than the current TOU rate. The electricity rates calculated for the workplace and residential area also exhibited different patterns. It is noteworthy that the highest TOU rate is allocated at 7 am in case of the workplace as shown in Fig. 6 despite the EVs are still arriving as shown in Fig. 5(a). Intuitively, one might think that the TOU rate at 7 am should be switched to the one at 3 am where no EV has arrived yet. However, if the TOU rates of both timeslots are switched, we observed that the peak load is increasing and even the profit of the aggregator is decreasing. This observation supports the necessity of the proposed method.

The net charging/discharging power of the V2G CS for the workplace and residential area are shown in Fig. 7(a) and (b), respectively. When the current TOU rate was applied to both locations, the ERO layer consumed the maximum amount of power ($200 \times 50 = 10{,}000$ kW). This suggests that the current TOU rate is completely ineffective in decreasing the capacity of power equipment. However, by applying the

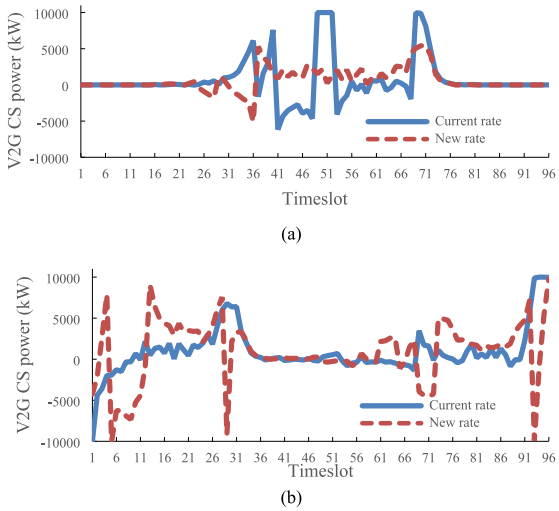

Fig. 7. Net charging/discharging power of V2G CS. (a) Workplace. (b) Residential area.

new TOU rates to the workplace and residential area, the ERO layer only consumed peak loads of 5,445 and 9,775 kW, respectively. This demonstrates that applying the newly produced rate from the optimization reduces the maximum power capacity for the V2G CS by around 54 % of the overall power rating of the EV chargers. However, it also shows that depending on the EV arrival/departure time distribution, the peak load will barely be reduced.

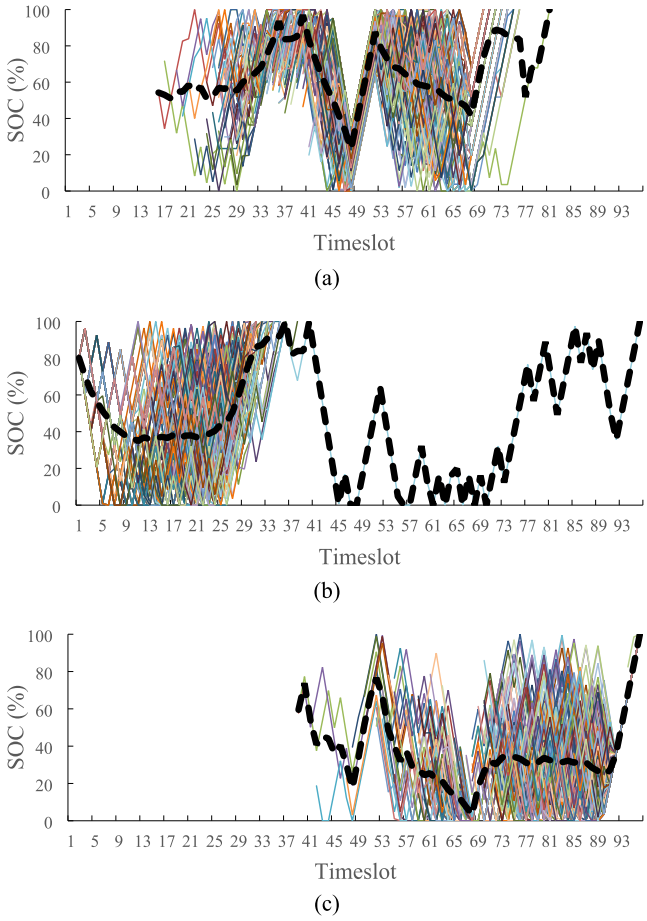

Fig. 8. SOC of EVs applying current TOU rate. (a) The workplace. (b) The residential area for the EVs connected since previous day. (c) The residential area for the newly arrived EVs. (Thick dashed line denotes the average SOC of all connected EVs).

The SOC results for the current and new TOU rates are shown in Figs. 8 and 9, respectively. The lines on the figures appear when the EVs are connected and disappear when the EVs are disconnected. Fig. 8(a) and 9(a) show the results for the workplace, and Fig. 8(b) and 9(b) are the results for the residential EVs that had been connected since the previous day. In order to present the tendency of SOC of 200 EVs more clearly, we added thick, dashed line to represent the average SOCs of all connected EVs. The figures show that one of the EVs, which lasts even after 41st timeslot, connected since the previous day remained connected until the end of the day, which is plausible in the real world. Fig. 8(c) and 9(c) show the results for the residential EVs that had newly arrived in the intraday period.

Table 5 shows the discomfort costs, which illustrate the proportion of the SOCs of the EVs that could not be fully charged before the EVs leave. For the workplace, all 200 EVs were fully charged. For the residential area, only one EV could not be fully charged, as it stayed at the CS for only 30 min. Thus, about 26.18 % of the SOC, which is equivalent to 5,236 KRW in terms of the discomfort cost, could not be charged.

The maximum profit made by the EV aggregator, as calculated by the EAO layer, is shown in Table 6. While calculating the EV aggregator's profit, we did not consider the profit share with EV owners since the aggregators' contract terms with their customers vary widely and continuously change [41]. So, the profit shown here is the profit before the aggregator share it with EV owners. One would expect the profit to decrease when the maximum power usage is minimized. Especially in case of the workplace, the profit is profoundly decreased down to only 1 % of that of the current TOU rate while using the new TOU rate. The profit can be increased by adjusting the electricity selling price. How much should the selling price be is left as a future work since it is out of scope of the paper as mentioned in Section 2. On the other hand, it is noteworthy that the profit is increased ten times in case of the residential area with the new TOU rate compared to that of the current TOU rate. So, in spite of negligible change of the peak load, the proposed optimization framework is still useful for a significant improvement of the EV aggregator's profit. In summary, the EV arrival/departure time distribution profoundly affects both peak load reduction and the profit of EV aggregator. Since the EV charging station peak load, EV arrival/departure time, TOU rate, and EV aggregator's profit are interrelated complicatedly, the regulator has to consider all of them to determine TOU rates for EV charging station.

5. Discussion and conclusion

Exploding EV sales will have a substantial impact on the capacity limit of distribution networks and necessitate the upgrading of transmission infrastructure. However, expanding the capacity of the power

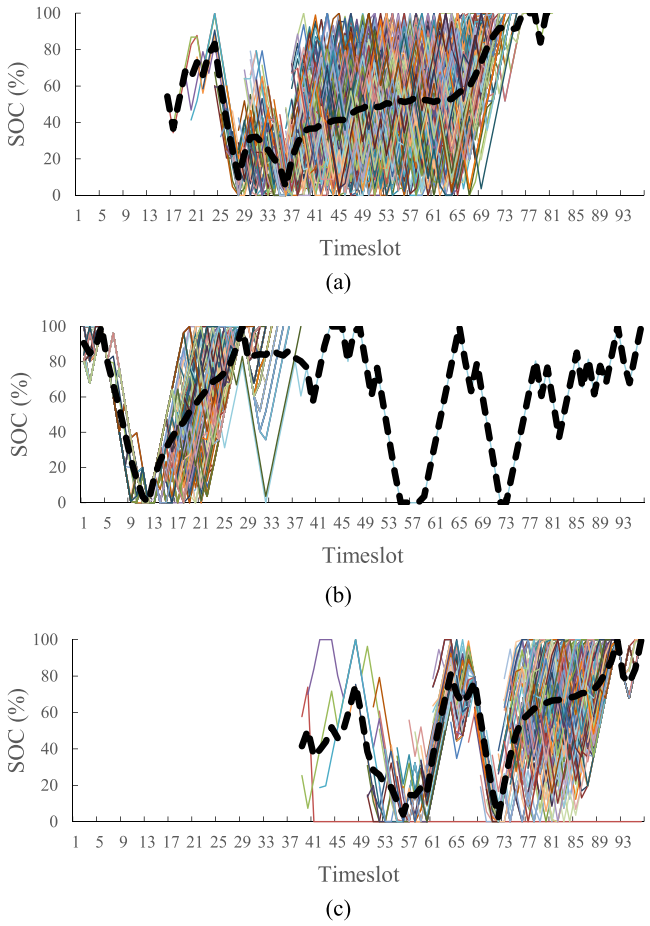

Fig. 9. SOC of EVs applying new TOU rate. (a) The workplace. (b) The residential area for the EVs connected since previous day. (c) The residential area for the newly arrived EVs. (Thick dashed line denotes the average SOC of all connected EVs).

Table 5
Discomfort costs.

V2G CS	Current TOU Rate	New TOU Rate
Workplace	0 KRW	0 KRW
Residential area	5,236 KRW	5,236 KRW

Table 6
Profits of EV aggregator.

V2G CS	Current TOU Rate	New TOU Rate
Workplace	1,404,840 KRW	8,824 KRW
Residential area	221,852 KRW	2,237,390 KRW

system infrastructure is extremely expensive. Moreover, the social cost, which is unquantifiable, must also be considered. To avoid upgrading the power capacity, we emphasize that the TOU electricity rate for EVs should be applied according to the EV arrival and departure time distributions of the V2G CS, as opposed to the peak demand of the whole power system, as is currently the case for utilities. Additionally, our results show that the installation power capacity can be reduced considerably by reducing the peak load of the CS, whereas the reduction in profit rate of the EV aggregator and the peak load of the CS vary significantly, depending on the EV arrival/departure time distribution, via the development and utilization of optimization framework. Although the EV aggregator's revenue is lowered, the maximum power capacity is reduced significantly, resulting in a reduction in V2G CS installation costs and an increase in social benefit owing to the deferral of power system infrastructure extension. However, the reduction of the profit of EV aggregator could be profound depending on the EV arrival/departure time distribution. The profit reduction could be compensated by adjusting the level of electricity selling price. The results from the simulation give new insight into the V2G CS business model in terms of the maximum installation capacity, TOU rate, and EV arrival/departure time distribution.

The ERO layer is employed here to compute the new TOU electricity rate; notably, some practical considerations for the EAO layer are overlooked. For example, the EV arrival and departure time distributions are configured to be deterministic; however, in practice, the EV arrival and departure timings always have a certain probability. The stochastic approach must be researched to provide a new TOU rate for future works.

CRediT authorship contribution statement

Jung-Sung Park: Writing – original draft, Resources, Project administration. **Shahid Hussain:** Writing – review & editing, Data curation, Conceptualization. **Jin-Oh Lee:** Software, Methodology, Investigation. **Balho H. Kim:** Validation, Supervision. **Yun-Su Kim:** Writing – review & editing, Project administration, Methodology, Funding acquisition, Conceptualization.

Declaration of competing interest

The authors declare that they have no known competing financial interests or personal relationships that could have appeared to influence the work reported in this paper.

Data availability

No data was used for the research described in the article.

Acknowledgements

This work was supported by the National Research Foundation of Korea (NRF) grant funded by the Korea government(MSIT) (No. 2022R1C1C1008910) and also supported by a Korea Institute of Energy Technology Evaluation and Planning (KETEP) grant funded by the Korean government (MOTIE) (No. RS-2023-00237679).

Appendix A

Since heuristic optimization algorithms such as PSO and GA are used, obtaining the global optimum is not guaranteed. As a result, the solution derived from such methods cannot be confirmed to be the global optimum. To demonstrate the efficiency of the modified PSO algorithm, we created a simple example problem with the following objective function:

$$\min_{r\in\mathscr{R}} \sum_{m=0}^{23} mr \tag{A1}$$

subject to (6). The global optimum for (A1) is $0 \times 2 + 1 \times 2 + \ldots + 5 \times 2 + 6 \times 1 + \ldots 13 \times 1 + 14 \times 0 + \ldots 23 \times 0 = 106$. Since the total number of m and number of control variables r equals to N^{var}, and because the constraints are the same as for the ERO layer, the effectiveness of the heuristic optimization for the ERO layer can be proven indirectly by applying them to (A1).

References

[1] Wappelhorst S. Update on government targets for phasing out new sales of internal combustion engine passenger cars. ICCT, Washington, DC, US. [Online]; 2021, Jun. Available: https://theicct.org/wp-content/ uploads/2021/12/update-govt-targets-ice-phaseouts-jun2021_0.pdf.

[2] Oda T, Aziz M, Mitani T, Watanabe Y, Kashiwagi T. Mitigation of congestion related to quick charging of electric vehicles based on waiting time and cost–benefit analyses: a Japanese case study. Sustain Cities Soc 2018;36:99–106.

[3] BIS Research. Electric vehicle fast-charging system market - A global and regional analysis: focus on DC fast charging applications, vehicle type, connector type, and power output of the DC charger system - Analysis and forecast, 2021-2031. Research and Markets, Dublin, Ireland. [Online]; 2022, Mar. Available: https://www.researchandmarkets.com/reports/5567756.

[4] Korea Electric Power Corporation (KEPCO). Terms of use for transmission and distribution electric power equipment. KEPCO, KR. [Online]; 2021, Oct. Available: https://cyber.kepco.co.kr/ckepco/front/jsp/CY/H/C/CYHCHP00704.jsp.

[5] Korea Power Exchange (KPX). Substation equipment. Electric power statistics information system. [Online]; 2022, Nov. Available: http://epsis.kpx.or.kr/epsisnew/selectEkfaTstChart.do?menuId=050200.

[6] Korea Expressway Corporation (KEC). Traffic volume of whole section. Expressway public data portal. [Online]; 2022, Nov. Available: http://data.ex.co.kr/visual/main.

[7] Wall DL, Parametric estimating for early electric substation construction cost. M.S. thesis, Dept. of Engineering Management, The University of Texas at Austin, Austin, TX; 2009.

[8] Park YG, Roh JH, Park JB, Choi MS, Kim GW, Kim JS. Economic evaluations of the alternatives to increase the supply capacity for large customers in the distribution systems. Trans Korean Inst Elect Eng 2011;60:500–8.

[9] Lopes JAP, Soares FJ, Almeida PMR. Integration of electric vehicles in the electric power system. Proc IEEE 2011;99:168–83.

[10] Ministry of Land Infrastructure and Transport, Korea Government. Cumulative number of registered car has reached 25,350,000. Press Release. [Online]; 2022, Oct. Available: http://www.molit.go.kr/USR/NEWS/ m_71/dtl.jsp?lcmspage=1&id=95087362.

[11] Tayarani H, et al. Optimal charging of plug-in electric vehicle: Considering travel behavior uncertainties and battery degradation. Appl Sci 2019;9:3420.

[12] Mohsenian-Rad H, Ghamkhari M. Optimal charging of electric vehicles with uncertain departure times: a closed-form solution. IEEE Trans Smart Grid 2015;6:940–2.

[13] Malisani P, Zhu J, Pognant-Gros P. Optimal charging scheduling of electric vehicles: the co-charging case. IEEE Trans Power Syst 2023;38:1069–80.

[14] Morstyn T, Crozier C, Deakin M, McCulloch MD. Conic optimization for electric vehicle station smart charging with battery voltage constraints. IEEE Trans Transp Electrif 2020;6:478–87.

[15] Gan L, Topcu U, Low SH. Optimal decentralized protocol for electric vehicle charging. IEEE Trans Power Syst 2013;28:940–51.

[16] Li Z, Gua Q, Sun H, Xin S, Wang J. A new real-time smart-charging method considering expected electric vehicle fleet connections. IEEE Trans Power Syst 2014;29:3114–5.

[17] Mahmud K, Hossain MJ, Town GE. Peak-load reduction by coordinated response of photovoltaics, battery storage, and electric vehicles. IEEE Access 2018;6:29353–65.

[18] Alam MJE, Muttaqi KM, Sutanto D. A controllable local peak-shaving strategy for effective utilization of PEV battery capacity for distribution network support. IEEE Trans Ind Appl 2015;51:2030–6.

[19] Şengör İ, Erdinç O, Yener B, Taşcikaraoğlu A, Catalão JPS. Optimal energy management of EV parking lots under peak load reduction based DR programs considering uncertainty. IEEE Trans Sustain Energy 2018;10:1034–43.

[20] Zhang G, Tan ST, Wang GG. Real-time smart charging of electric vehicles for demand charge reduction at non-residential sites. IEEE Trans Smart Grid 2018;9:4027–37.

[21] Casini M, Vicino A, Zanvettor GG. A receding horizon approach to peak power minimization for EV charging stations in the presence of uncertainty. Int J Electric Power Energy Syst 2021;126:106567.

[22] Davis BM, Bradley TH. The efficacy of electric vehicle time-of-use rates in guiding plug-in hybrid electric vehicle charging behavior. IEEE Trans Smart Grid 2012;3:1679–86.

[23] Honarmand M, Zakariazadeh A, Jadid S. Integrated scheduling of renewable generation and electric vehicles parking lot in a smart microgrid. Energy Conv Manag 2014;86:745–55.

[24] Ren H, Zhang A, Wang F, Yan X, Li Y, Duić N, et al. Optimal scheduling of an EV aggregator for demand response considering triple level benefits of three-parties. Int J Electric Power Energy Syst 2021;125:106447.

[25] Yan L, Ai X, Wang Y, Zhang H. Impacts of electric vehicles on power grid considering time series of TOU. In: Proc. ITEC Asia-Pacific; 2014. p. 1–5.

[26] Erdinç O, Taşcikaraoğlu A, Paterakis NG, Dursun İ, Sinim MC, Catalão JPS. Comprehensive optimization model for sizing and siting of DG units, EV charging stations, and energy storage systems. IEEE Trans Smart Grid 2018;9:3871–82.

[27] Mozafar MR, Maradi MH, Amini MH. A simultaneous approach for optimal allocation of renewable energy sources and electric vehicle charging stations in smart grids based on improved GA-PSO algorithm. Sust Cities Soc 2017;32:627–37.

[28] Xiong Y, Gan J, An B, Miao C, Bazzan ALC. Optimal electric vehicle fast charging station placement based on game theoretical framework. IEEE Trans Intell Transp Syst 2018;19:2493–504.

[29] Islam MM, Shareef H, Mohamed A. Optimal location and sizing of fast charging stations for electric vehicles by incorporating traffic and power networks. IET Intell Transp Syst 2018;12:947–57.

[30] Sharma I, Cañizares C, Bhattacharya K. Smart charging of PEVs penetrating into residential distribution systems. IEEE Trans Smart Grid 2014;5:1196–209.

[31] Hua L, Wang J, Zhou C. Adaptive electric vehicle charging coordination on distribution network. IEEE Trans Smart Grid 2014;5:2666–75.

[32] Chen N, Tan CW, Quek TQ. Electric vehicle charging in smart grid: optimality and valley-filling algorithms. IEEE J Sel Topics Signal Process 2014;8:1073–83.

[33] Sarker MR, Ortega-Vazquez MA, Kirschen DS. Optimal coordination and scheduling of demand response via monetary incentives. IEEE Trans Smart Grid 2015;6(3):1341–52.

[34] Veldman E, Verzijlbergh RA. Distribution grid impacts of smart electric vehicle charging from different perspectives. IEEE Trans Smart Grid 2015;6:333–42.

[35] Kim J, Bialek S, Unel B, Dvorkin Y. Strategic policymaking for implementing renewable portfolio standards: a tri-level optimization approach. IEEE Trans Power Syst 2021;36:4915–27.

[36] Boyd S, Vandenberghe L. Convex functions. In: Convex Optimization, 7th printing with corrections. Cambridge, UK: Cambridge University Press; 2009.

[37] Korea Electric Power Corporation (KEPCO) Electricity tariff structure. KEPCO, KR. [Online]; 2022, Oct. Available: https://cyber.kepco.co. kr/ckepco/front/jsp/CY/E/E/CYEEHP00108.jsp.

[38] Muller RA. The energy landscape. In: Energy for future presidents: the science behind the headlines, Reprint ed., New York, NY, USA: W. W. Norton & Company; 2013.

[39] Kennedy J, Eberhart R. Particle swarm optimization. In: Proc. ICNN; 1995. p. 1942–8.

[40] National Household Travel Survey (NHTS). [Online]; 2023, Dec. Available: https://nhts.ornl.gov/.

[41] DNV. The regulation of independent aggregators with a focus on cmpensation mechanisms, Nordic Energy Research 2022, [Online]; 2022, Apr. Available: https://www.nordicenergy.org/publications/the-regulation-of-independent-aggregators-with-a-focus-on-compensation-mechanisms/.